

pubs.acs.org/JPCC Article

# Frontier Orbital Degeneracy: A New Concept for Tailoring the Magnetic State in Organic Semiconductor Adsorbates

Anubhab Chakraborty, Percy Zahl, Qingqing Dai, Hong Li, Torsten Fritz, Paul Simon, Jean-Luc Brédas, and Oliver L. A. Monti\*



Cite This: J. Phys. Chem. C 2023, 127, 23504–23515



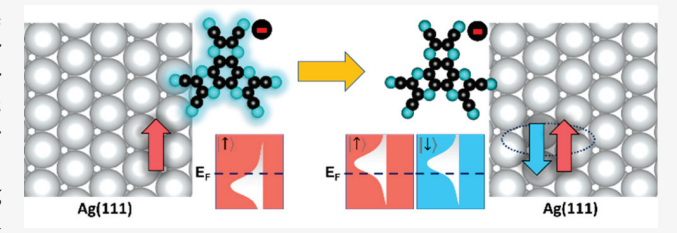
**ACCESS** 

III Metrics & More

Article Recommendations

s Supporting Information

**ABSTRACT:** Kondo resonances in molecular adsorbates are important building blocks for applications in the field of molecular spintronics. Here, we introduce the novel concept of using frontier orbital degeneracy for tailoring the magnetic state, which is demonstrated for the case of the organic semiconductor 1,4,5,8,9,11-hexaazatriphenylenehexacarbonitrile (HATCN,  $C_{18}N_{12}$ ) on Ag(111). Low-temperature scanning tunneling microscopy/spectroscopy (LT-STM/STS) measurements reveal the existence of two types of adsorbed HATCN molecules with



distinctly different appearances and magnetic states, as evident from the presence or absence of an Abrikosov–Suhl–Kondo resonance. Our DFT results show that HATCN on Ag(111) supports two almost isoenergetic states, both with one excess electron transferred from the Ag surface but with magnetic moments of either 0 or 0.65  $\mu_{\rm B}$ . Therefore, even though all molecules undergo charge transfer of one electron from the Ag substrate, they exist in two different molecular magnetic states that resemble a free doublet or an entangled spin state. We explain how the origin of this behavior lies in the 2-fold degeneracy of the lowest unoccupied molecular orbitals of gas phase HATCN, lifted upon adsorption and charge-transfer from Ag(111). Our combined STM and DFT study introduces a new pathway to tailoring the magnetic state of molecular adsorbates on surfaces, with significant potential for spintronics and quantum information science.

#### ■ INTRODUCTION

The highly versatile electronic structure of organic semiconductors has brought increasing attention in recent years to their potential application in the field of spintronics. <sup>1–6</sup> The diversity of readily accessible molecular scaffolds and ease of synthesis of derivatives allow precise control over the electronic structure, adsorption geometry, and extent of wave function coupling of these molecules to different substrates. <sup>7–9</sup> This is crucial for tuning the electronic and magnetic interactions at the interface of molecular thin films on surfaces. <sup>10</sup> These underlying interactions are key to controlling the charge and spin states of molecules and offer an opportunity for designing molecular spintronic devices.

At the atomic or molecular scale, electronic correlations and many-body interactions are of great importance, particularly when considering the spin degree of freedom. A notable manifestation of such correlations is the Kondo effect, a many-body effect that arises from the coupling of a localized spin moment of an adsorbate to the electron spins in the conduction band of a metal substrate. <sup>11–14</sup> This gives rise to a singlet ground state due to screening of the localized spin moment by an itinerant cloud of spins from the Fermi sea of the substrate. <sup>15</sup> The signature of such Kondo screening is the appearance of a narrow resonance in the density of states

(DOS) near the Fermi level, known as the Abrikosov–Suhl–Kondo (ASK) resonance. 14,16

Original work on Kondo systems was concerned with transport anomalies in dilute magnetic alloys, <sup>11</sup> quantum dot systems, <sup>17–20</sup> and magnetic impurities; <sup>13,21</sup> however, in recent years, organic semiconductors adsorbed on coinage metal surfaces <sup>22–27</sup> have emerged as promising alternatives in this field because of their versatile chemical and electronic structures, consequently creating a rich parameter space for tailoring electronic correlations at interfaces. Multiple studies have explored the effects of chemical structure, <sup>24,28</sup> magnetic state of transition metal complexes, <sup>27,29,30</sup> adsorption geometry, <sup>22,31</sup> and self-assembly <sup>32,33</sup> in molecular Kondo systems. Particularly promising is the prospect of tailoring magnetic states in such systems, with initial attempts demonstrated in recent reports. <sup>22,23,30,34,35</sup> In all of these works, transitions between the molecular doublet state and the molecule/substrate coupled singlet state have been achieved by

Received: October 6, 2023
Revised: November 3, 2023
Accepted: November 5, 2023
Published: November 20, 2023





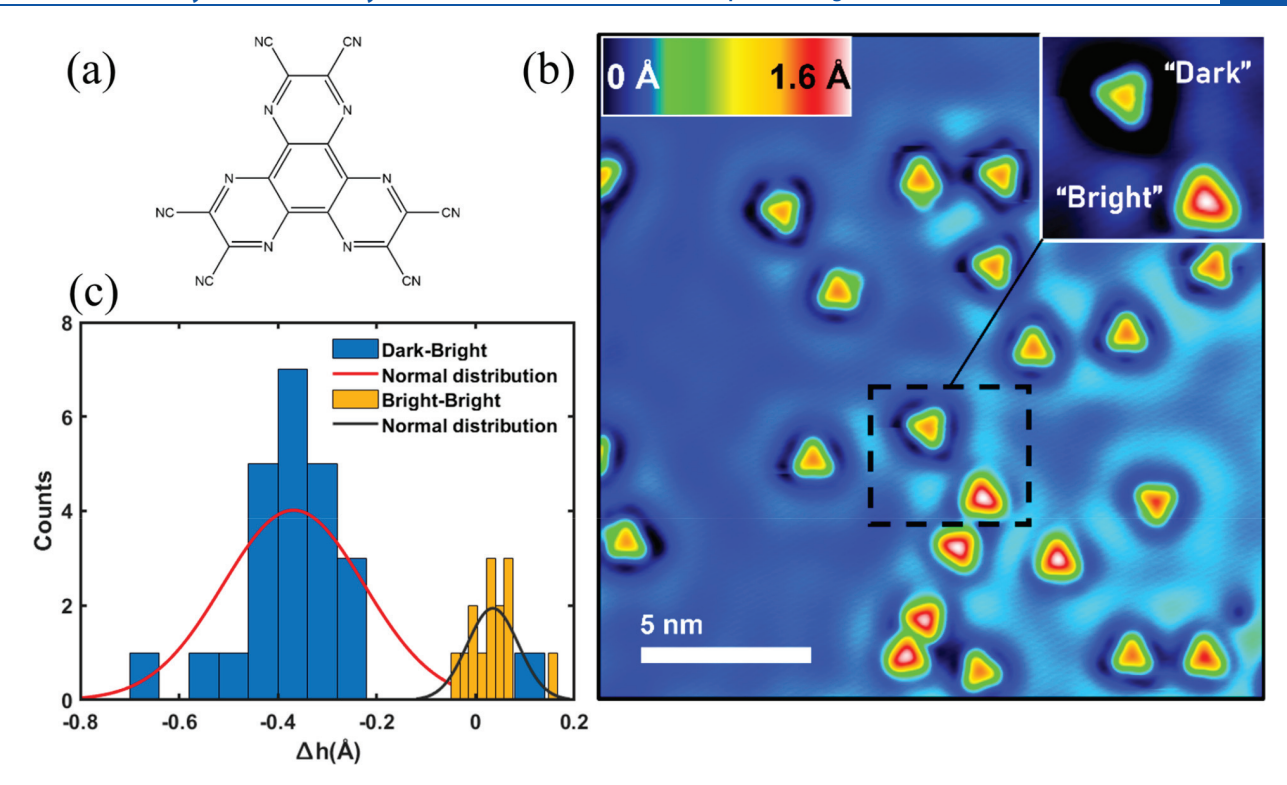


Figure 1. (a) Molecular structure of HATCN. (b) Constant current STM image of HATCN molecules adsorbed on the Ag(111) surface at 5 K (0.2 V, 0.01 nA). The inset shows a close-up of the two types of appearances. (c) Histograms showing the STM height difference ( $\Delta h$ ) between pairs of "Bright" and "Dark" types (blue) and pairs of "Bright" and "Bright" types (orange). Fits by normal distributions to the histograms are shown in red and black and indicate an average  $\Delta h$  of 0.37(2) and 0.03(1) Å, respectively.

manipulating the adsorption geometry or by modifying the chemical or electronic structure of the adsorbate molecule. The ability to *design* a molecular adsorbate system that is able to support both the molecular doublet state and the entangled Kondo singlet without chemical modification remains however an open problem.

Here, we introduce a novel and likely general approach to meet this challenge: We show that an organic adsorbate whose frontier orbitals are degenerate can readily support multiple nearly isoenergetic magnetic states. We use scanning tunneling microscopy and spectroscopy (STM and STS) of the organic semiconductor HATCN on Ag(111) together with density functional theory (DFT) to show that such magnetic bistability, observed clearly from the presence/absence of an ASK resonance, is intrinsic to this system due to the degeneracy of the lowest unoccupied molecular orbital of HATCN in the gas phase. Our work provides a novel concept to tailor magnetic states and a new way to understand molecular Kondo systems. The insight that the frontier orbital degeneracy and symmetry of the molecule can open a door to access different magnetic states and hence to tailor magnetic states unlocks new types of Kondo systems potentially suited for applications such as building blocks for nanospintronic/ low-dimensional spintronic devices, <sup>36,37</sup> spin-state transfer in extended systems, <sup>38</sup> using chains of nonzero spin molecules to drive on-chain oligomerization, 39,40 as well as in information storage and computing by making use of tailored spin states 41-43 in molecular adsorbates.

## METHODS

**Sample Preparation.** Ag(111) was cleaned by using Ar<sup>+</sup> sputtering (1 keV, 5  $\mu$ A/cm<sup>2</sup>) and annealing (823 K).

Commercially acquired HATCN (Alfa Chemistry, 99.5%) was purified by three cycles of gradient sublimation (573 K) in a custom-built furnace. The UHV system base pressure was  $7 \times 10^{-10}$  Torr. HATCN molecules were directly deposited on the cold (5 K) Ag surface by flashing a small amount from a silicone carrier substrate that was heated by a direct current. Film thickness is reported in terms of monolayer equivalent (MLE) as a fraction of a hypothetical monolayer (ML) on the Ag(111) substrate held at 5 K, with 1 ML  $\approx 5.6 \times 10^{13}$  molecules/cm<sup>2.44</sup> The last preparation step was exposing the sample to a small CO dose, while, at 5 K, specifically 10 s of CO exposure at 2  $\times$  10<sup>-8</sup> mbar is required for tip functionalization purposes only.

STM-STS-AFM. 0.1 MLE HATCN/Ag(111). Measurements were performed with a Createc-based low-temperature (LT)-STM system custom upgraded with HR-AFM capability and operated using the open source GXSM control software. HR-AFM measurements were performed using GXSM's special constant height control mode with automated constant current (STM mode) transitions if a compliance setting (probe safety or also automated big/3D molecule lift mode) of a maximum allowed tunnel current is exceeded. A small bias of 20 mV was typically applied in HR-AFM-mode. For frequency detection, the custom, high-speed GXSM RedPitaya-PAC-PLL controller was used.

STS was performed by using an external Lock-In Amplifier (SRS Model 7265 Dual Phase DSP Lock-in Amplifier). The bias was modulated at 299 Hz at typically 10 or 5 mV pure sine amplitude. Other experimental parameters such as imaging conditions, stabilization point (bias voltage and tunneling current), and sample temperature are specified where necessary.

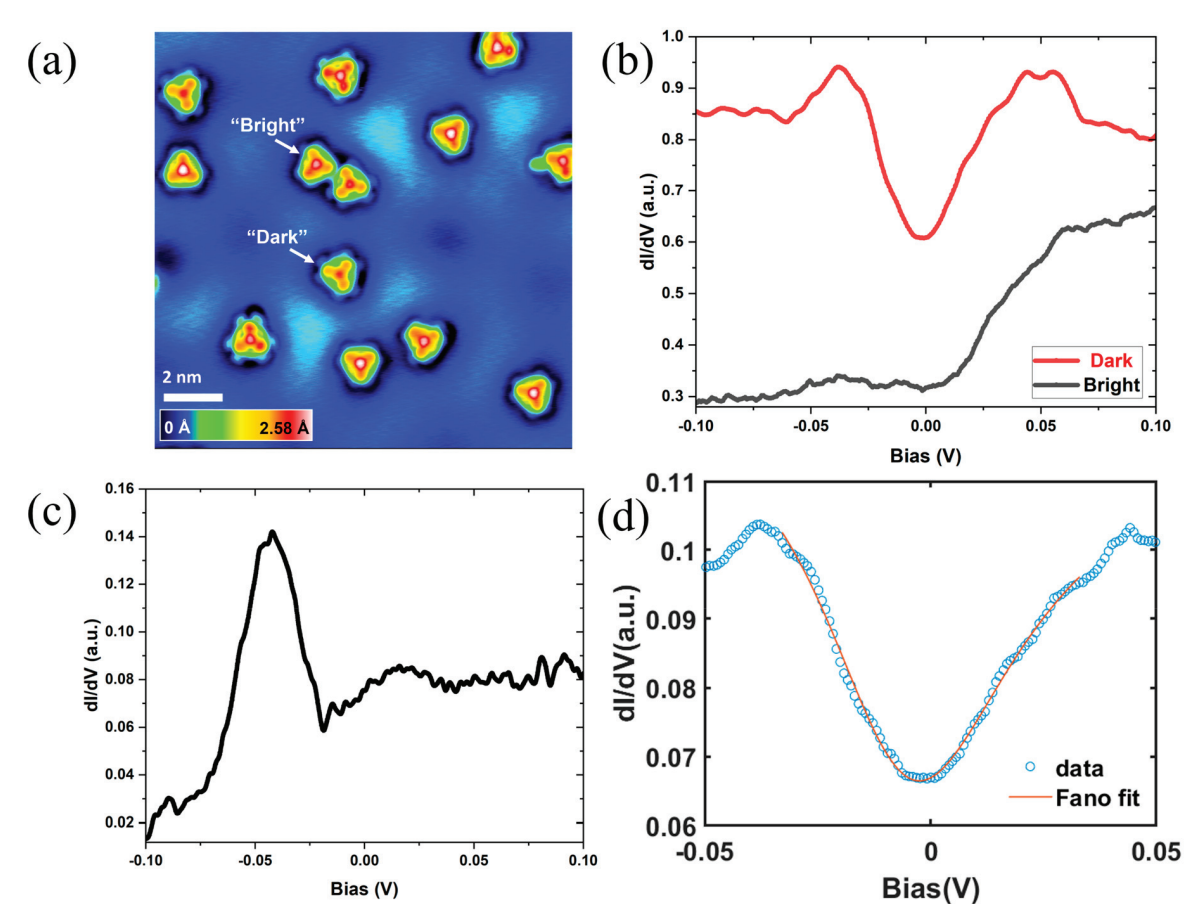


Figure 2. (a) Constant current STM at 5 K (0.04 V, 2 pA) showing some of the molecules for which STS measurements were performed. (b) STS scan of molecules labeled in (a) demonstrating the existence of an antiresonance feature for the "Dark" molecules and centered at -1 meV, in contrast to the unstructured spectrum for the "Bright" molecules. The red and black curves shown in (b) are typical  $\frac{dI}{dV}$  spectra for "Dark" and "Bright" molecules, respectively. (c)  $\frac{dI}{dV}$  spectrum of the Ag(111) substrate. (d)  $\frac{dI}{dV}$  spectrum and Fano fit for the "Dark" molecule in (b), with  $E_0 = -1(1)$  meV,  $\Gamma = 51(1)$  meV, and Q = -0.1(1).

1 ML HATCN/Ag(111). STM and STHM measurements of HATCN layers on Ag(111) were performed with a JT-STM/AFM system from SPECS Surface Nano Analysis using a mechanically cut PtIr tip. The STM system is operated with a Nanonis SPM controller (ver. 5) featuring an integrated lockin amplifier that we used for the STS experiments. Here, a typical modulation voltage of 6 mV with a tip lift of 1 nm was set. The working temperature was 4.5 K. The STS spectrum shown in Figure 4b was taken as an average of several measurements from one STS map of a HATCN layer. Triplicate measurements were made at 11 molecular centers on different HATCN molecules and averaged. The averaging was done independently. Additional experimental parameters are given where necessary.

**DFT.** Spin-polarized density functional theory (SDFT) calculations were carried out using the projector augmented wave (PAW) method<sup>48</sup> as implemented in VASP. The Ag(111) surface was modeled by five-layer slabs with the bottom three layers fixed at the bulk Ag structures and the top two layers relaxed; the HATCN/Ag interfaces were modeled by a supercell consisting of  $7 \times 7$  Ag(111) primitive cells and by considering adsorption sites of a HATCN molecule on hollow-fcc, hollow-hcp, top, and bridge sites. The Ag(111)—HATCN slabs were separated by a vacuum space of about 40 Å. To compensate for any long-range dipole—dipole

interactions among the asymmetric slabs across the vacuum space, the dipole-correction approach as implemented in VASP was also applied. In the initial screening of all adsorption sites, the Perdew-Burke-Ernzerhof (PBE) functional was used with DFT-D3<sup>51</sup> dispersion corrections; once the most stable adsorption site (hollow FCC) was found, the PBE functional with density-dependent energy corrections (dDsC)<sup>52,53</sup> was applied in further geometry optimizations and subsequent electronic-structure calculations. In all calculations, a cutoff energy of 500 eV was considered for the plane-wave basis set. A  $\Gamma$ -point only k-mesh and a 5  $\times$  5  $\times$  1 Monkhorst-Pack kmesh were used in the geometry optimizations and electronicstructure calculations, respectively. In the structure optimizations, the atomic positions were relaxed until the forces on each atom were smaller than 0.01 eV/Å and the energies converged to 10<sup>-6</sup> eV. A Bader (for DFT-D3 corrections) or Hirshfeld (for dDsC corrections) analysis was adopted to evaluate the charge transfer from the Ag(111) surface to the HATCN. Simulations of constant-current STM images were carried out in the framework of the Tersoff-Hamann approximation.54,55

# ■ RESULTS AND DISCUSSION

**Observations.** We start by presenting a summary of the key findings obtained from scanning probe microscopy of

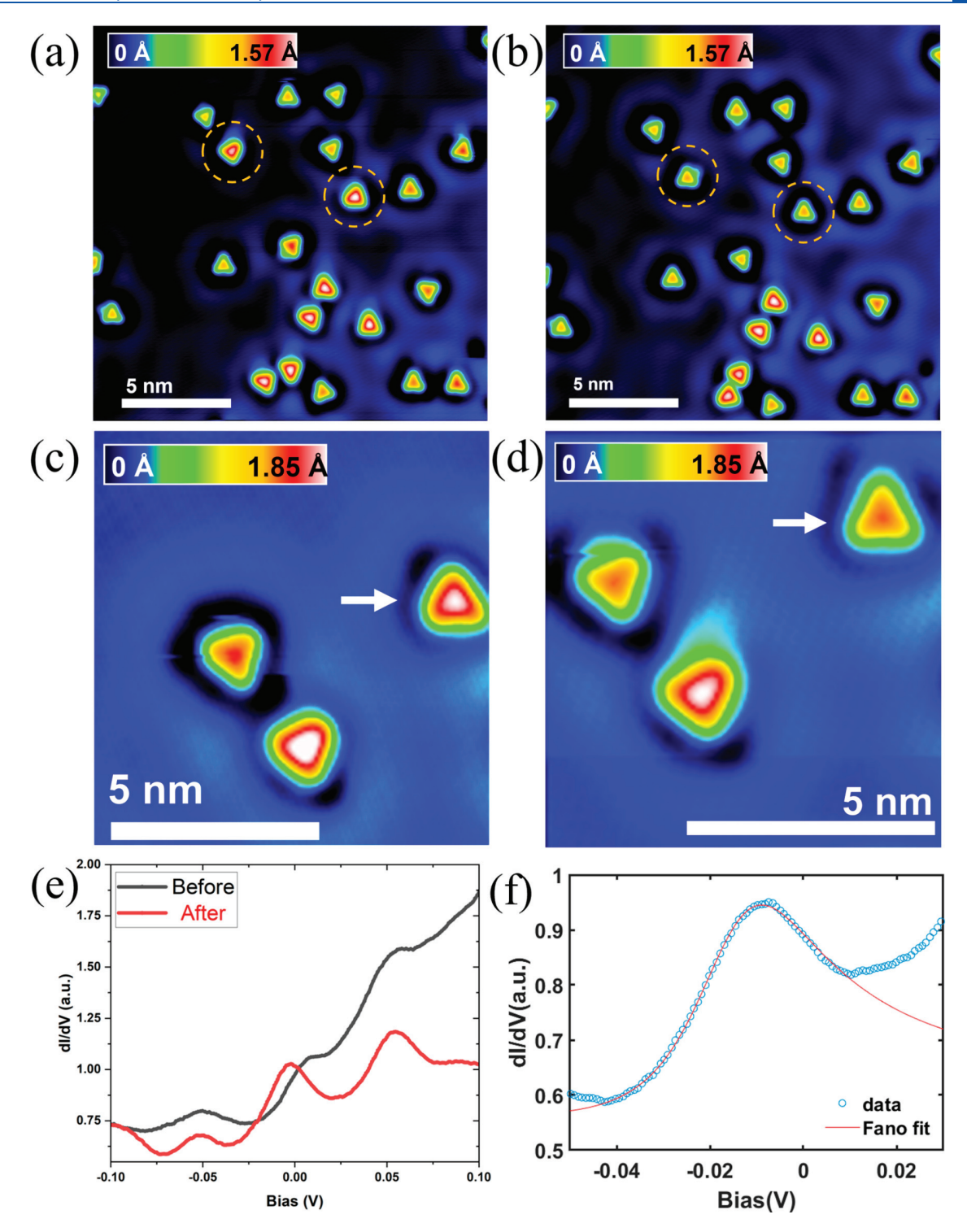


Figure 3. Constant current STM images (0.2 V, 0.01 nA) (a, c) before and (b, d) after switching of highlighted molecules. (e)  $\frac{dI}{dV}$  spectra of the highlighted molecule in (c) and (d) before and after switching. (f) Fano fit for the "after" spectrum (red curve) shown in (e), with  $E_0 = -12(1)$  meV,  $\Gamma = 38(1)$  meV, and Q = -0.2(1).

HATCN on Ag(111). A 0.1 monolayer equivalent (MLE, see the Methods section) of HATCN molecules (molecular structure displayed in Figure 1a) adsorbed on a Ag(111) surface at 5 K shows two distinct types of contrast in constant current STM images (Figure 1b): Molecules either have a bright center (labeled "Bright") or a less bright center (labeled "Dark", inset in Figure 1b) (see also Figure S1, Supporting

Information). These contrast differences are tip—sample bias independent (see Figure S1, Supporting Information), and their appearance in this imaging mode is otherwise identical. Analysis of 50 pairs of HATCN molecules shows that, on average, the STM height of "Bright" molecules is 0.37(2) Å higher than that of "Dark" molecules (Figure 1c). Though we note that this height difference is an apparent height difference

only, convoluted with the z-dependence of the tunneling matrix element, <sup>56–58</sup> we conclude from this and many other images that there are two and only two distinct molecular "types" of HATCN on Ag(111), distinguished *qualitatively* by their appearance contrasts ("Bright" or "Dark") and *quantitatively* by their apparent STM heights (see Figure S2, Supporting Information).

To gain insight into the origin of the STM contrast differences, differential conductance (dI/dV) spectroscopy was performed. The dI/dV spectra measured over a wide range of biases and acquired on the central benzene ring of HATCN (Figure 2a) show a distinctive narrow resonance/antiresonance near the Fermi energy  $E_{\rm F}$  (i.e., bias of 0 V) in the case of "Dark" molecules (typical cases shown in Figure 2b). This is distinctly different from the unstructured spectra near  $E_{\rm F}$  for the Ag(111) surface local DOS (LDOS) (Figure 2c). Interestingly, this zero-bias feature is exclusively observed in "Dark" molecules and is absent in "Bright" molecules (Figure 2a,b). Analysis of dI/dV spectra for 60 molecules shows a 98% correlation between the molecule "type" and the appearance of a zero-bias feature in STS. As discussed in detail later, we interpret this narrow zero-bias resonance/antiresonance, observed only on the "Dark" HATCN molecules, as a characteristic fingerprint of the Kondo effect, a result of screening in the HATCN/Ag(111) many-body system that manifests as an Abrikosov-Suhl-Kondo (ASK) resonance in transport measurements. 14,16,21,59-62 The requirement for the observation of an ASK resonance is the existence of unpaired electrons on the adsorbate, as is the case for HATCN: It accepts close to one full electron upon adsorption on Ag(111).63,64 The line shape of the ASK resonance is described well by a Fano function, though other functional forms have been proposed as well.<sup>65,66</sup> This functional form considers the interfering pathways of (i) direct tunneling between the tip and Ag(111) surface and (ii) tunneling mediated through the Kondo impurity (i.e., a HATCN molecule in the "Dark" state); 13,65,67,68 we use this model to fit the experimental dI/dV spectra

$$\frac{\mathrm{d}I}{\mathrm{d}V} = \frac{C(q+\varepsilon)^2}{1+\varepsilon^2} + \rho_0 \tag{1}$$

where  $\varepsilon = \frac{\epsilon V - E_0}{\Gamma}$ ,  $E_0$  is the resonance energy,  $2\Gamma$  is the full width at half-maximum (fwhm) of the resonance, q is the dimensionless coupling parameter between the magnetic impurity and the continuum states of the tip or the Ag substrate, and  $\rho_0$  is the background differential conductance. Analysis of dI/dV spectra for 35 HATCN molecules of "Dark" type gives  $E_0$  and  $\Gamma$  values of -7(1) and 38(1) meV, respectively. The values of q range between  $\pm 1$ , likely due to different tip conditions between scans which lead to different tip-surface coupling (see Section S3, Supporting Information), and indicate a significant role of the quantum interference. This is reflected in different peak shapes for the observed ASK resonance on the "Dark" HATCN molecules, as well as slight variations in the precise articulation of the HATCN appearance in the constant current STM images (see Figure S3, Supporting Information).<sup>68–70</sup> The observation of different shapes for the zero-bias feature in different STS spectra (compare, for example, Figure 2b and Figure 3e) suggests that this is indeed an ASK resonance in the coupled HATCN/Ag(111) system and not a spectral feature of either HATCN or Ag(111). From the ASK resonance widths, the

Kondo temperature is estimated to be 231 K. Note that, with such a high estimated Kondo temperature, a temperature-dependent STS study in the range of 5–50 K would not change appreciably the ASK resonance width. A magnetic-field-dependent study of these ASK features would be interesting, since it would allow estimating the exchange interaction. This is however outside the scope of the present report.

The small  $E_0$  and narrow fwhm of the resonance are signatures of the ASK resonance and imply that "Dark" molecules act as spin-flip scattering centers embedded in the sea of silver conduction electrons. Since the Kondo effect arises due to an interaction between an unpaired spin of an impurity with the physically neighboring electron sea, <sup>11,22,69,71</sup> we deduce that "Dark" molecules have an unpaired spin (s=1/2) while "Bright" molecules do not (s=0). This then points to the key feature of our system: the *magnetic bistability* of HATCN on Ag(111), which we define as the coexistence of two nearly isoenergetic states with different magnetic configurations.

This is a remarkable finding for a molecular adsorbate system such as HATCN/Ag(111), since it is only correlated with the apparent height and not with the adsorption geometry, as we will also show later computationally. Previous studies have reported the tunable control and activation of the Kondo effect in molecular adsorbate systems on metal substrates. This is usually achieved by using coordination chemistry between molecular units and paramagnetic atomic ions such as transition metals to create molecular alloys with intrinsic magnetic moments, <sup>22,26–29,35,71–73</sup> or by modifying the adsorption geometry of molecules using external stimuli such as voltage pulses, <sup>23,24,26,31</sup> temperature (via annealing), <sup>22</sup> or even molecular structure manipulation using an STM tip. <sup>24,26</sup> The present system is unique in this regard since the magnetic bistability is intrinsic to the system and does not require external stimulus or the presence of paramagnetic components.

Having established the existence of two magnetic states and consequently two distinct STM contrasts, we now demonstrate the ability of HATCN molecules to switch from a "Bright" to a "Dark" state. Parts a and b of Figure 3 show an example of this effect: Observed in successive STM scans, we find that "Bright" molecules switch stochastically to the "Dark" state; this switching is unidirectional, always going from "Bright" to "Dark". It is important to mention that this is not a result of a significant displacement or rotation of the molecule, as evident from before and after STM scans and DFT calculations (vide infra). The switching is also not dependent on STM imaging conditions, which is confirmed by taking scans at different tip sample biases and set point currents. Both molecular "Types" are observed within the bias range of  $\pm 0.3$  V, and even under a high bias of 2.0 V (see Figure S1, Supporting Information), suggesting that local electric fields do not cause switching. Further, this is not a heat-induced effect either, as the sample was held at a constant 5 K throughout the measurements. We return to the nature of this switching later in this paper. Most importantly, the only change upon switching is of the molecular magnetic state, with no change of the adsorption geometry.

To relate the change in appearance to the magnetic state of the molecule, we carried out differential conductance measurements on molecules that undergo switching. We observe that a switch from "Bright" to "Dark" (Figure 3c,d) is indeed

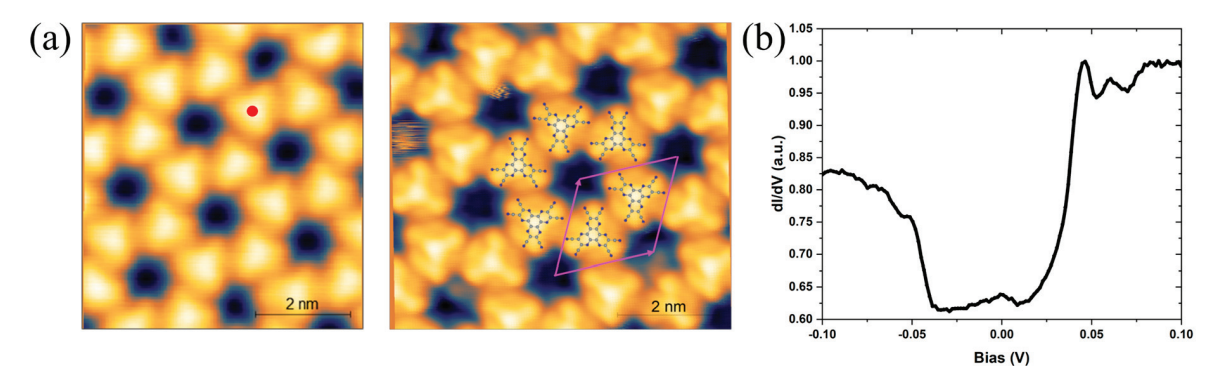


Figure 4. (a) Constant current STM (left) (-0.4 V, 400 pA, 4.5 K) and STHM (right) (-0.5 V, 30 pA, 4.5 K) of a close-packed HATCN layer on Ag(111) showing the honeycomb structure. The colored red dot indicates the position where the  $\frac{dI}{dV}$  spectrum shown in (b) was measured.

accompanied by the appearance of a zero-bias Kondo resonance in the  $\mathrm{d}I/\mathrm{d}V$  spectra (Figure 3e, red curve), as expected for a change in the magnetic state. This implies that molecules can switch from a nonmagnetic (s=0) to a magnetic state (s=1/2). Fitting the  $\mathrm{d}I/\mathrm{d}V$  spectra for this particular molecule (Figure 3c,d) with the Fano model gives  $E_0=-12(1)$  meV,  $\Gamma=38(1)$  meV, and q=-0.2(1) (Figure 3f), consistent with the observed distribution of values for "Dark" molecules.

Origin of Magnetic Bistability. To study whether the Kondo effect in the HATCN/Ag(111) system is limited to single molecules or can also be found in close-packed molecular layers and to understand its origin, we also investigated the electronic structure and appearance by LT-STM and Scanning Tunneling Hydrogen Microscopy (STHM) in ordered molecular monolayers. As reported already,  $^{44,63,64}$  HATCN forms well-ordered layers on Ag(111) that exhibit a honeycomb structure (Figure 4a) with 6 HATCN molecules arranged in a ring with a commensurate 7  $\times$  7 alignment (see Figure S5, Supporting Information).

For STS measured in the center of molecules in such a layer (same as for isolated HATCN molecules), we exclusively found spectra similar to those in Figure 2b and Figure 3e of the "Bright" state (black curves), i.e., without Kondo resonance (Figure 4b). We note that there is a very weak peak near 0 V for these molecules (Figure 4b), which does, however, not resemble the pronounced Fano-shaped features found in isolated "Dark" molecules. While the true nature of this small peak and another peak at +50 mV remains unknown, we speculate that these two features are related to the splitting of the doubly degenerate LUMO of isolated HATCN, with the lower level now partially occupied and the upper level sitting at +50 mV in both isolated and densely packed molecules. These features are caused by integer charge transfer from the Ag substrate irrespective of the molecular magnetic state (see computational results below). Also visible in these spectra is a peak around -50 mV which represents the surface state of Ag(111) (cf. the STS curve of the bare Ag substrate in Figure 2c; see also Figure S6, Supporting Information).

We confirm therefore that the mere existence of a radical on a surface, while necessary, is not sufficient for observing a Kondo resonance. From those findings, we conclude also that the Kondo effect is indeed limited to single molecules and does not occur in well-ordered honeycomb structures. Apparently, molecule—molecule interactions in the layers, either directly or substrate mediated, hinder the Kondo effect. This suggests that

there exists a subtle balance between the two molecular states, "Dark" and "Bright" or Kondo and no Kondo. This is a further indication of the near-degeneracy of the involved levels.

To understand the origin of this balance, we performed spinpolarized density functional theory (SDFT) calculations for the HATCN/Ag(111) system. Geometry optimizations indicate that the cyano groups are bent toward the substrate, causing a significant buckling of the molecule. Based on Hirshfeld charge analyses (when using the dDsC dispersion corrections, see the Methods section) and Bader charge analyses (when using DFT-D3 dispersion corrections, see the Methods section), the HATCN molecule accepts ~1 electron from Ag(111) upon chemisorption, irrespective of the adsorption site or orientation on the surface. These findings are in line with previous works 44,64 and demonstrate that even "Bright" molecules are expected to have undergone charge transfer from Ag(111). Our SDFT calculations reveal the existence of two and only two different equilibrium spin configurations, in excellent agreement with our experimental observations of "Bright" and "Dark" molecules. We label these as "Charge Transfer (CT) Doublet" and "Charge Transfer (CT) Singlet". The two configurations are very similar (see Table 1) in terms of their total energies ( $\Delta E = 10 \text{ meV}$ ) and

Table 1. Properties of the Spin Configurations in HATCN/Ag(111) from SDFT Calculations

| Configuration            | Relative Energy (meV) | Magnetic Moment/ $\mu_{\rm B}$ | Charge Transfer<br>(Hirshfeld) |
|--------------------------|-----------------------|--------------------------------|--------------------------------|
| CT Doublet<br>("Dark")   | 0                     | 0.65                           | 0.98                           |
| CT Singlet<br>("Bright") | +10                   | ~0                             | 0.96                           |

the charge accepted from Ag(111) ( $\sim$ 1 electron), which confirms that both types remain indeed radicals. We note that these results do not depend on the adsorption site. Remarkably, the "CT Doublet" configuration has a magnetic moment of 0.65  $\mu_{\rm B}$ , in contrast to that of the "CT Singlet" configuration ( $\sim$ 0  $\mu_{\rm B}$ ). This suggests that only the "CT Doublet" configuration, which is slightly more stable, is able to support an ASK resonance, while the "CT Singlet" configuration is overall nonmagnetic despite its radical character. This interpretation is further supported by the spin-resolved projected density of states (PDOS), where the spin polarization of HATCN is maintained in the "CT Doublet" configuration with a split spin-resolved PDOS near  $E_{\rm F}$  (Figure 5a, red curves). Indeed, a spin-up singly occupied

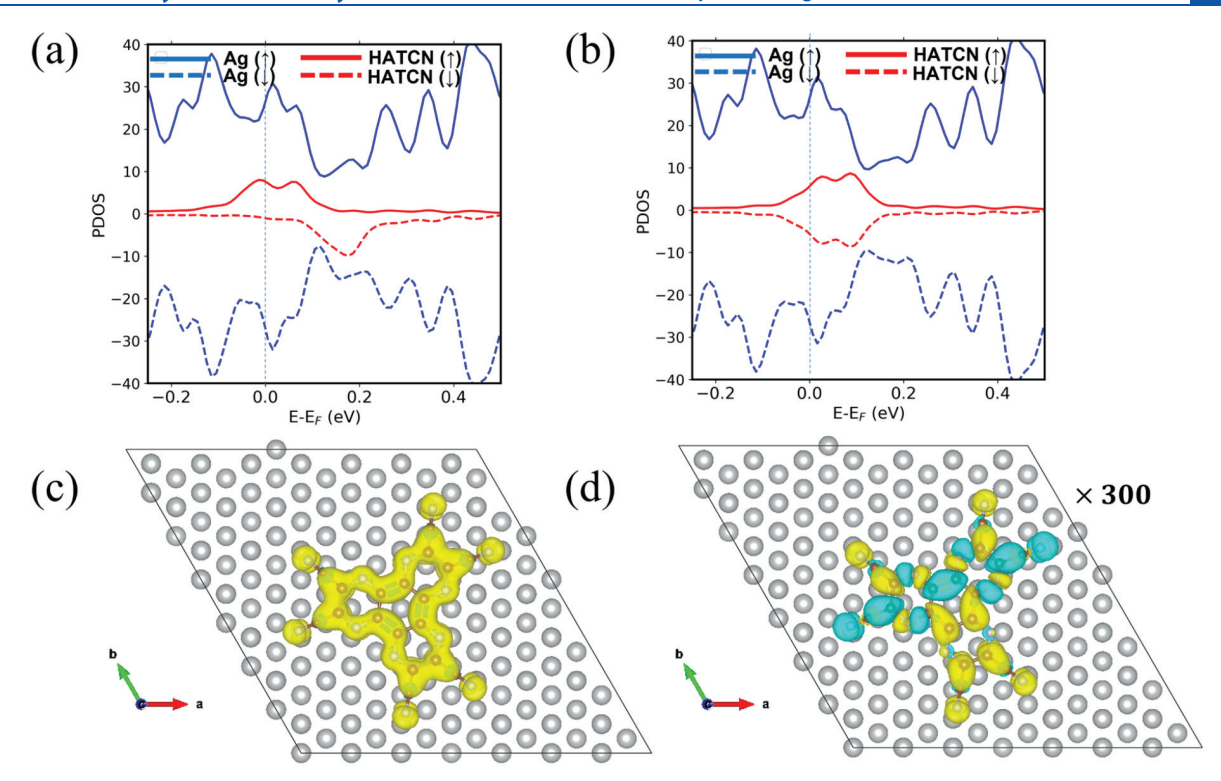


Figure 5. PDOS of HATCN/Ag(111) for (a) CT doublet and (b) CT singlet configurations. Blue plots represent the Ag PDOS; red plots represent the HATCN PDOS. Spin-up ( $\uparrow$ ) and spin-down ( $\downarrow$ ) channels are shown using solid and dashed lines, respectively. Spin density plots for (c) CT doublet and (d) CT singlet configurations, with the isosurface value in (d) being 2 orders of magnitude smaller than that in (c).

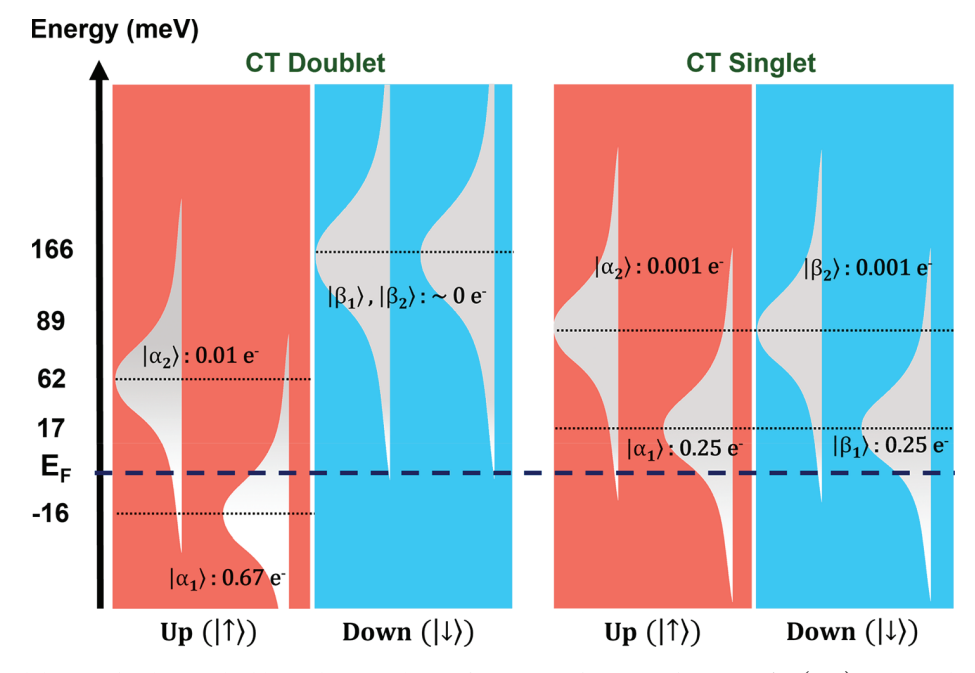


Figure 6. Energy level diagram for the CT doublet and CT singlet configurations of 0.1 ML of HATCN/Ag(111) near  $E_{\rm F}$ , obtained from fitting the calculated HATCN PDOS (red curves in Figure 5a,b). The indices 1 and 2 refer to the two nondegenerate former LUMOs of adsorbed HATCN, while  $\alpha$  and  $\beta$  represent the spin-up and the spin-down channels, respectively. Red and blue boxes show the single electron states for spin-up and spin-down channels, respectively. In addition, the electron charge below  $E_{\rm F}$  is shown for each state.

molecular orbital (SOMO) sits right at  $E_{\rm F}$ , while the spin-down orbital is nearly completely unoccupied. In contrast, for the "CT Singlet" configuration, the PDOS corresponding to the spin-up and spin-down states is nearly degenerate and straddling  $E_{\rm F}$  (Figure 5b, red curves). We note that the features near 0 eV in the PDOS plot for HATCN correspond

to the HATCN SOMO and do not represent the ASK resonance observed in the dI/dV spectra since these DFT calculations cannot account for the many-body physics at play in the Kondo effect. However, the calculations demonstrate a salient feature of the magnetic bistability in this system: The spin associated with the excess electron accepted by HATCN

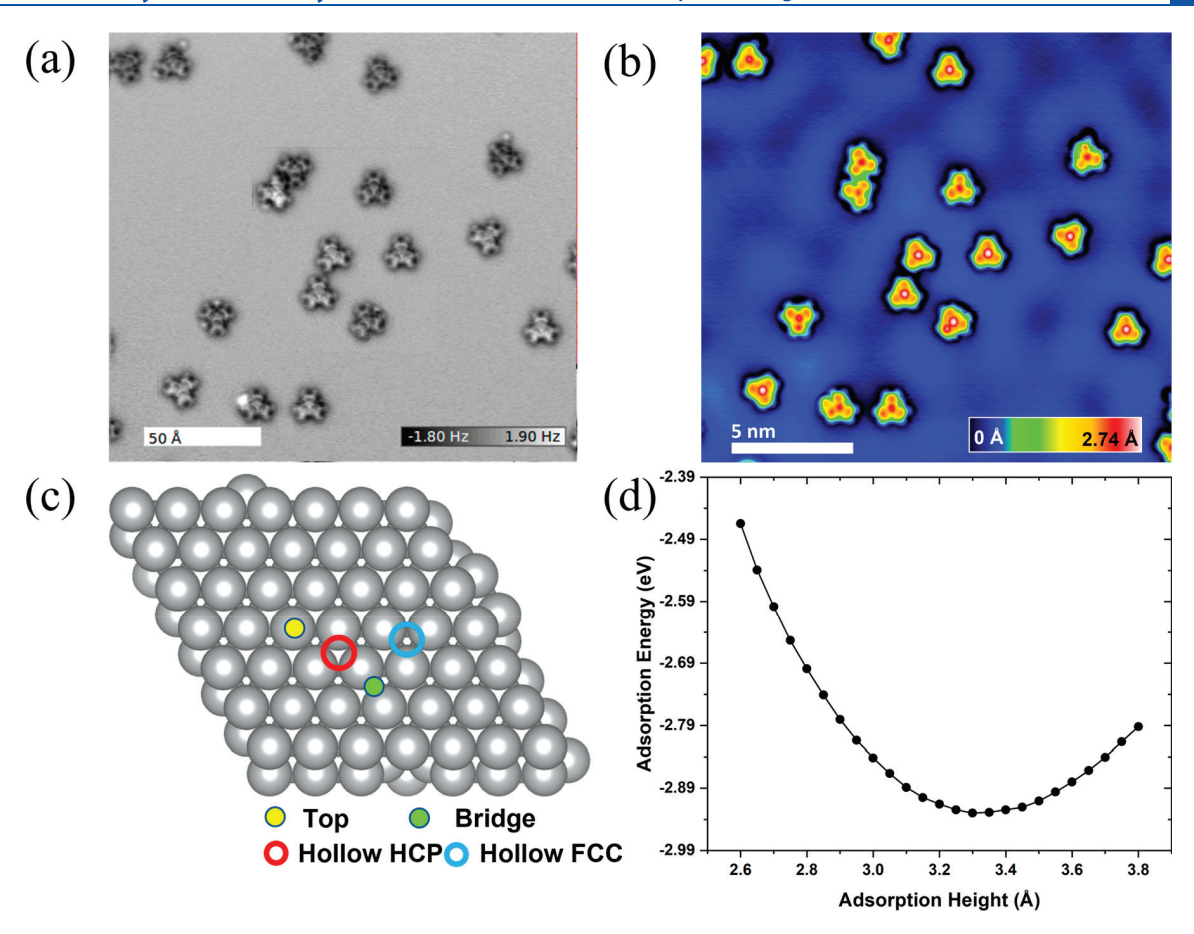


Figure 7. (a) Constant height HR-AFM (0.02 V) and (b) constant current STM at 5 K (0.05 V, 2 pA) images taken over the same region. The contrast seen in (b) showing the two types cannot be observed in (a). (c) Adsorption sites on Ag(111) considered in our DFT calculations. (d) DFT calculated adsorption energy profile for the hollow FCC site. The minimum of 3.3 Å corresponds to the adsorption height of HATCN on Ag(111).

from Ag(111) can be arranged in two different ways: (i) either "Up" ( $|\uparrow\rangle$ ) or "Down" ( $|\downarrow\rangle$ ), which gives rise to an ASK resonance and the "Dark" molecules, or (ii) in a superposition of "Up" and "Down" ( $|\uparrow\rangle + |\downarrow\rangle$ ) with net magnetic moment equal to zero and without an ASK resonance, which is responsible for the "Bright" molecules.

The associated spin densities for these configurations are plotted in Figure 5c and d and demonstrate the presence of an electron spin delocalized over the whole molecule for the more stable "CT Doublet" version of the molecule, supportive of the observation of an ASK resonance. In contrast, the spin density for the "CT Singlet" molecule is nearly zero (note that the spin isosurface value is nearly 3 orders of magnitude smaller in Figure 5d than that in Figure 5c). As a consequence, even though this molecular adsorbate has also undergone electron transfer of nearly a full electron, spin entanglement leads to a net zero spin polarization and hence the absence of a prominent ASK resonance.

To understand this phenomenon in more detail, we further analyzed the spin-resolved HATCN PDOS (Figure 5a,b) to extract the energies of the molecular states near  $E_{\rm F}$  (Figure 6). For this analysis, we fit the HATCN PDOS with two Gaussians per spin channel, allowing the 2-fold degeneracy of the LUMO in an isolated HATCN molecule to be lifted upon adsorption on Ag(111) and acceptance of an electron from the substrate (see Figure S7 and Section S10, Supporting Information). From the area under the curve below  $E_{\rm F}$ , we obtain the

electronic charge for each spin. It is clear from this simple analysis that, even though the total electronic charge below  $E_{\rm E}$ is similar for both the CT Doublet (0.67 + 0.01 = 0.68 e) and CT Singlet (0.50 e) configurations, the distribution of this total charge across different MOs is quite different in each case. As evident in Figure 6, for the CT Doublet, the charge resides in the spin-up channel ( $|\alpha\rangle$ ) and in fact mostly in the  $|\alpha 1\rangle$  state, leading to spin polarization. In contrast, the spin-up  $(|\alpha\rangle)$  and spin-down ( $|\beta\rangle$ ) channels remain degenerate for the CT Singlet configuration, and the total charge is distributed equally and almost entirely in the  $|\alpha_1\rangle$  and  $|\beta_1\rangle$  states. This leads to spin entanglement and net zero spin polarization. Note that these extracted charges are in reasonable agreement with the Hirshfeld charges, particularly considering that they are obtained from a simple model of PDOS near  $E_{\rm F}$ . This energy level diagram is also consistent with the experimentally obtained energies of HATCN/Ag(111) states. For instance, we can assign the features at +11 and +60 mV for the spectrum of the molecule "Before Switching" (or "Bright") (Figure 3e, black curve) as the CT Singlet  $|\alpha_1\rangle$  (or  $|\beta_1\rangle$ ) and the CT Singlet  $|\alpha_2\rangle$  (or  $|\beta_2\rangle$ ) states, respectively. For the spectrum of the molecule "After Switching" (or "Dark") (Figure 3e, red curve), the peaks at -12 and +54 mV are assigned to the ASK resonance and the CT Doublet  $|\alpha_2\rangle$  states, respectively. We emphasize once more that the features near 0 V for "Bright" HATCN molecules (Figure 3e) and molecules in close-packed layers (Figure 4b) are assigned to the CT Singlet  $|\alpha_1\rangle$  (or  $|\beta_1\rangle$ )

state and are not the ASK resonance observed in the  $\mathrm{d}I/\mathrm{d}V$  spectra of "Dark" HATCN molecules (see Section S6, Supporting Information).

To summarize, the key ingredients for the observed magnetic bistability stem from frontier orbital degeneracy, high molecular symmetry, and energetic proximity of the frontier molecular orbitals to the Fermi level, which lead to lifting of the degeneracy of the LUMO upon adsorption of HATCN on Ag(111) and charge transfer to the molecule. Spin-spin correlation interactions with the surface lead to small but crucial energetic differences and orbital occupancies, which manifest in fundamentally different magnetic states. Taken together, the STS and DFT results show that, because of the gas phase degeneracy of molecular frontier orbitals, there exist two energetically close-lying states with fundamentally different magnetic properties for isolated HATCN molecules on Ag(111). Indeed, previous studies have reported the presence of charge transfer induced ASK resonance in metal/organic systems exhibiting one or more of these conditions. <sup>25,74</sup> It is conceivable that the rather small energetic difference of 10 meV is compensated for by intermolecular interactions in HATCN films, hindering the observation of a Kondo resonance in that case.

We also note that the process of acquiring an STM image itself implies that, given the calculated small energy difference between the two configurations, switching by the STM tip, e.g., due to high electric fields in the tunnel junction, or spontaneous thermally activated switching is possible, consistent with our observations. Future studies of this system are needed to elucidate the exact mechanism of this switching, which is beyond the scope of the current work. Instead, we emphasize that the principal finding of this work is the existence of two magnetic states resulting from frontier orbital degeneracy in the HATCN/Ag(111) system.

To investigate the validity of these conclusions, we considered several alternative hypotheses. First, we considered different adsorption geometries leading to different electronic configurations as a possible explanation for our experimental observations. We performed high-resolution atomic force microscopy (HR-AFM) imaging on a HATCN/Ag(111) system. Notably, we do not find any correlation between the HR-AFM and STM contrasts (Figure 7a,b), indicating that whatever geometric differences may exist, including adsorption sites or a small rotation on the surface, these do not explain the difference between "Dark" and "Bright" molecules. In fact, there is no consistent contrast difference between different HATCN molecules in the HR-AFM images themselves (Figure 7a and Figure S11, Supporting Information) nor a correlation with the contrast differences seen in the STM scan (Figure 7b) to suggest the existence of two different HATCN adsorption geometries. HR-AFM provides information about chemical bonds and on-surface molecular structure, 26,75,76 and the lack of distinct differences correlated between STM and HR-AFM suggests that the origin of the two types cannot be based on different on-surface molecular structures. This is also in agreement with the fact that, from DFT geometry optimizations obtained at different adsorption sites of Ag(111) (Figure 7c), there is no strict molecule—surface registry, and many translationally and rotationally slightly different configurations exist (see Figure S4, Supporting Information). Importantly, these slightly different adsorption configurations all result in the same electronic structures and very similar magnetic moments (see Sections S8 and S9,

Supporting Information), unable to explain the origin of the differences between "Bright" and "Dark" molecules observed in LT-STM and dI/dV spectra. From these results, we can conclude that the occurrence of either "Type" does not depend on either the adsorption site or the molecular orientation (rotation), which for the case of isolated molecules on the surface is reflected in the disordered and seemingly random distribution of either "Type". We also note that the higher spatial resolution of HR-AFM helps to exclude adatoms or atoms sandwiched between the Ag(111) surface and HATCN as potential causes of the observed contrasts and different magnetic properties. Processes such as hydrogenation of HATCN leading to magnetic moment changes are also unlikely given our experimental conditions (10-10 mbar, 5 K), which favor neither the kinetics nor the thermodynamics of such reactions.

Second, we investigated the possibility of two adsorption height minima in the adsorption energy. A hypothetical additional minimum at a slightly larger height could trap molecules in a metastable site, likely with different electronic properties and molecule—surface coupling due to the expected weaker electronic coupling to the substrate. Under the influence of an electric field or over time, one would expect that such molecules escape this first minimum to reach the thermodynamic minimum on the surface. Our DFT calculations (Figure 7d) unambiguously show, however, that there are no other minima in the adsorption energy profile; <sup>31,34</sup> the two STM contrasts are therefore not caused by metastable adsorption geometries. Instead, the different STM apparent heights are primarily reflective of two different electronic structures and indeed magnetic states.

Taken together, our DFT calculations indicate that the origin of the distinct STM contrasts cannot be explained by differences in the HATCN adsorption on Ag(111). The combined results from DFT and HR-AFM strongly suggest that adsorption induced structural or electronic differences are minimal for the HATCN/Ag(111) system.

# CONCLUSIONS

We close by highlighting the significance of our findings. The Kondo effect in molecular adsorbate systems has conventionally been manipulated by altering either the electronic structure or the adsorption geometry of the adsorbate species. The novelty of the HATCN/Ag(111) system presented here is that neither of these methods is required to support two different magnetic states on the surface. Instead, we propose that this kind of magnetic bistability and switching results from lifting of the frontier orbital degeneracy upon adsorption, and will be manifested in molecular systems with a minimum of 2-fold degeneracy near  $E_{\rm F}$ , provided the energy level alignment with the metal substrate facilitates charge transfer. In fact, bidirectional switching might be possible at room temperature because of the energetic closeness of the CT Doublet and CT Singlet states as well as the estimated high Kondo temperature.

More broadly, the ability of the HATCN anion radical to exhibit two completely different spin distributions with only a small energy difference is quite intriguing and may allow for the creation of a Kondo lattice by preferentially "pushing" the molecule to one or the other magnetic state. Lastly, our results provide deeper insight into the Kondo effect by considering the spin density distribution and associated magnetic moments for all supported configurations in the radical species instead of only connecting the effect to the extra electronic charge. Our

work therefore opens avenues for precise control of molecular Kondo switches, creation of Kondo lattices, and tailoring of surface—adsorbate interactions in organic semiconductor interfaces.

#### ASSOCIATED CONTENT

# Supporting Information

The Supporting Information is available free of charge at https://pubs.acs.org/doi/10.1021/acs.jpcc.3c06656.

STM images, STM heights, adsorption geometries of HATCN/Ag(111), STS spectra, LEED, gas phase and on-surface DFT calculations, PDOS plots for different adsorption sites, fits for CT doublet and singlet states, STM simulations, HR-AFM, and STM comparison (PDF)

# AUTHOR INFORMATION

### **Corresponding Author**

Oliver L. A. Monti — Department of Chemistry and Biochemistry and Department of Physics, University of Arizona, Tucson, Arizona 85721, United States; orcid.org/0000-0002-0974-7253; Phone: (+1) 520 626 1177; Email: monti@arizona.edu

#### **Authors**

Anubhab Chakraborty — Department of Chemistry and Biochemistry, University of Arizona, Tucson, Arizona 85721, United States; orcid.org/0000-0002-1902-8308

Percy Zahl — Center for Functional Nanomaterials, Brookhaven National Laboratory, Upton, New York 11973, United States; Occid.org/0000-0002-6629-7500

Qingqing Dai – Department of Chemistry and Biochemistry, University of Arizona, Tucson, Arizona 85721, United States

Hong Li − Department of Chemistry and Biochemistry, University of Arizona, Tucson, Arizona 85721, United States; © orcid.org/0000-0002-4513-3056

Torsten Fritz — Department of Chemistry and Biochemistry, University of Arizona, Tucson, Arizona 85721, United States; Institute of Solid State Physics, Friedrich Schiller University Jena, 07743 Jena, Germany; ocid.org/0000-0001-6904-1909

Paul Simon – Institute of Solid State Physics, Friedrich Schiller University Jena, 07743 Jena, Germany

Jean-Luc Brédas — Department of Chemistry and Biochemistry, University of Arizona, Tucson, Arizona 85721, United States; Ocid.org/0000-0001-7278-4471

Complete contact information is available at: https://pubs.acs.org/10.1021/acs.jpcc.3c06656

## **Author Contributions**

Anubhab Chakraborty: conceptualization, data curation, formal analysis, investigation, methodology, writing—original draft. Percy Zahl: data curation, investigation, methodology, resources, software, funding acquisition. Qingqing Dai: data curation, investigation. Hong Li: data curation, investigation, methodology, resources. Torsten Fritz: funding acquisition, project administration, resources, supervision, validation, writing—review and editing. Paul Simon: data curation, investigation. Jean-Luc Brédas: funding acquisition, project administration, resources, supervision, validation. Oliver L. A. Monti: conceptualization, funding acquisition, project administration, project administration, funding acquisition, project administration, project administration, funding acquisition, project administration.

istration, resources, supervision, validation, writing—review and editing.

#### Notes

The authors declare no competing financial interest.

#### ACKNOWLEDGMENTS

This research was supported by the National Science Foundation under Grant No. NSF CHE-1954571 and by the College of Science of the University of Arizona. This research also used the LT-STM/HR-AFM facility of the Center for Functional Nanomaterials (CFN), which is a U.S. Department of Energy Office of Science User Facility, at Brookhaven National Laboratory under Contract No. DE-SC0012704. We also thank The University of Arizona - UA CBC Laboratory for Electron Spectroscopy and Surface Analysis (LESSA) Facility (RRID:SCR\_022885) for this research.

#### REFERENCES

- (1) Joshi, V. K. Spintronics: A contemporary review of emerging electronics devices. *Engineering Science and Technology, an International Journal* **2016**, 19, 1503–1513.
- (2) Dieny, B.; Prejbeanu, I. L.; Garello, K.; Gambardella, P.; Freitas, P.; Lehndorff, R.; Raberg, W.; Ebels, U.; Demokritov, S. O.; Akerman, J.; et al. Opportunities and Challenges for Spintronics in the Microelectronics Industry. *Nat. Electron.* **2020**, *3* (8), 446–459.
- (3) Bandyopadhyay, S.; Cahay, M. Introduction to Spintronics, 2nd ed.; CRC Press: Boca Raton, FL, 2015.
- (4) Sun, D.; Ehrenfreund, E.; Valy Vardeny, Z. The First Decade of Organic Spintronics Research. *Chem. Commun.* **2014**, *50* (15), 1781–1793.
- (5) Prinz, G. A. Magnetoelectronics. *Science* **1998**, 282 (5394), 1660–1663.
- (6) Wolf, S. A.; Awschalom, D. D.; Buhrman, R. A.; Daughton, J. M.; von Molnár, S.; Roukes, M. L.; Chtchelkanova, A. Y.; Treger, D. M. Spintronics: A Spin-Based Electronics Vision for the Future. *Science* **2001**, 294 (5546), 1488–1495.
- (7) Introducing Molecular Electronics, 1st ed.; Cuniberti, G., Richter, K., Fagas, G., Eds.; Lecture Notes in Physics; Springer: Berlin, Heidelberg, 2005.
- (8) Naber, W. J. M.; Faez, S.; van der Wiel, W. G. Organic Spintronics. J. Phys. Appl. Phys. 2007, 40 (12), R205–R228.
- (9) Cho, K.; Pak, J.; Chung, S.; Lee, T. Recent Advances in Interface Engineering of Transition-Metal Dichalcogenides with Organic Molecules and Polymers. ACS Nano 2019, 13 (9), 9713–9734.
- (10) Fahlman, M.; Fabiano, S.; Gueskine, V.; Simon, D.; Berggren, M.; Crispin, X. Interfaces in Organic Electronics. *Nat. Rev. Mater.* **2019**, 4 (10), 627–650.
- (11) Kondo, J. Resistance Minimum in Dilute Magnetic Alloys. *Prog. Theor. Phys.* **1964**, 32 (1), 37–49.
- (12) Child, T.; Cross, M.; Tully, A.; Werner, M. An Introduction to the Kondo Effect; 2018.
- (13) Madhavan, V.; Chen, W.; Jamneala, T.; Crommie, M. F.; Wingreen, N. S. Local Spectroscopy of a Kondo Impurity: Co on Au(111). *Phys. Rev. B* **2001**, *64* (16), No. 165412.
- (14) Scott, G. D.; Natelson, D. Kondo Resonances in Molecular Devices. ACS Nano 2010, 4 (7), 3560–3579.
- (15) Coleman, P. Introduction to Many-Body Physics; Cambridge University Press: Rutgers University, NJ, 2015.
- (16) Hewson, A. C. The Kondo Problem to Heavy Fermions; Cambridge University Press: Cambridge, U.K., 1997.
- (17) Jeong, H.; Chang, A. M.; Melloch, M. R. The Kondo Effect in an Artificial Quantum Dot Molecule. *Science* **2001**, 293 (5538), 2221–2223.
- (18) Pustilnik, M.; Glazman, L. Kondo Effect in Quantum Dots. J. Phys.: Condens. Matter 2004, 16 (16), R513-R537.

- (19) Sasaki, S.; De Franceschi, S.; Elzerman, J. M.; van der Wiel, W. G.; Eto, M.; Tarucha, S.; Kouwenhoven, L. P. Kondo Effect in an Integer-Spin Quantum Dot. *Nature* **2000**, 405 (6788), 764–767.
- (20) Hiraoka, R.; Minamitani, E.; Arafune, R.; Tsukahara, N.; Watanabe, S.; Kawai, M.; Takagi, N. Single-Molecule Quantum Dot as a Kondo Simulator. *Nat. Commun.* **2017**, *8* (1), 16012.
- (21) Ternes, M.; Heinrich, A. J.; Schneider, W.-D. Spectroscopic Manifestations of the Kondo Effect on Single Adatoms. *J. Phys.: Condens. Matter* **2009**, *21* (5), No. 053001.
- (22) Maughan, B.; Zahl, P.; Sutter, P.; Monti, O. L. A. Ensemble Control of Kondo Screening in Molecular Adsorbates. *J. Phys. Chem. Lett.* **2017**, *8* (8), 1837–1844.
- (23) Choi, T.; Bedwani, S.; Rochefort, A.; Chen, C.-Y.; Epstein, A. J.; Gupta, J. A. A Single Molecule Kondo Switch: Multistability of Tetracyanoethylene on Cu(111). *Nano Lett.* **2010**, *10* (10), 4175–4180.
- (24) Zhao, A.; Li, Q.; Chen, L.; Xiang, H.; Wang, W.; Pan, S.; Wang, B.; Xiao, X.; Yang, J.; Hou, J. G.; et al. Controlling the Kondo Effect of an Adsorbed Magnetic Ion Through Its Chemical Bonding. *Science* **2005**, 309 (5740), 1542–1544.
- (25) Granet, J.; Sicot, M.; Gerber, I. C.; Kremer, G.; Pierron, T.; Kierren, B.; Moreau, L.; Fagot-Revurat, Y.; Lamare, S.; Chérioux, F.; et al. Adsorption-Induced Kondo Effect in Metal-Free Phthalocyanine on Ag(111). *J. Phys. Chem. C* **2020**, *124* (19), 10441–10452.
- (26) Hellerstedt, J.; Cahlík, A.; Švec, M.; de la Torre, B.; Moro-Lagares, M.; Chutora, T.; Papoušková, B.; Zoppellaro, G.; Mutombo, P.; Ruben, M.; et al. On-Surface Structural and Electronic Properties of Spontaneously Formed Tb <sub>2</sub> Pc <sub>3</sub> Single Molecule Magnets. *Nanoscale* **2018**, *10* (33), 15553–15563.
- (27) Wahl, P.; Diekhöner, L.; Wittich, G.; Vitali, L.; Schneider, M. A.; Kern, K. Kondo Effect of Molecular Complexes at Surfaces: Ligand Control of the Local Spin Coupling. *Phys. Rev. Lett.* **2005**, *95* (16), No. 166601.
- (28) Soe, W.-H.; Robles, R.; de Mendoza, P.; Echavarren, A. M.; Lorente, N.; Joachim, C. Doublet-Singlet-Doublet Transition in a Single Organic Molecule Magnet On-Surface Constructed with up to 3 Aluminum Atoms. *Nano Lett.* **2021**, *21* (19), 8317–8323.
- (29) Idobata, Y.; Zhou, B.; Kobayashi, A.; Kobayashi, H. Molecular Alloy with Diluted Magnetic Moments—Molecular Kondo System. *J. Am. Chem. Soc.* **2012**, *134* (2), 871–874.
- (30) Kim, H.; Chang, Y. H.; Lee, S.-H.; Kim, Y.-H.; Kahng, S.-J. Switching and Sensing Spin States of Co-Porphyrin in Bimolecular Reactions on Au(111) Using Scanning Tunneling Microscopy. ACS Nano 2013, 7 (10), 9312–9317.
- (31) Kügel, J.; Karolak, M.; Krönlein, A.; Serrate, D.; Bode, M.; Sangiovanni, G. Reversible Magnetic Switching of High-Spin Molecules on a Giant Rashba Surface. *Npj Quantum Mater.* **2018**, 3 (1), 53.
- (32) Iancu, V.; Deshpande, A.; Hla, S.-W. Manipulation of the Kondo Effect via Two-Dimensional Molecular Assembly. *Phys. Rev. Lett.* **2006**, 97 (26), No. 266603.
- (33) Tsukahara, N.; Shiraki, S.; Itou, S.; Ohta, N.; Takagi, N.; Kawai, M. Evolution of Kondo Resonance from a Single Impurity Molecule to the Two-Dimensional Lattice. *Phys. Rev. Lett.* **2011**, *106* (18), No. 187201.
- (34) Liu, W.; Filimonov, S. N.; Carrasco, J.; Tkatchenko, A. Molecular Switches from Benzene Derivatives Adsorbed on Metal Surfaces. *Nat. Commun.* **2013**, *4* (1), 2569.
- (35) Inose, T.; Tanaka, D.; Liu, J.; Kajihara, M.; Mishra, P.; Ogawa, T.; Komeda, T. Coordination Structure Conversion of Protonated Bisporphyrinato Terbium(III) Double-Decker Complexes and Creation of a Kondo Assembly by Electron Injection on the Au(111) Surface. *Nanoscale* **2018**, *10* (41), 19409–19417.
- (36) DiLullo, A.; Chang, S.-H.; Baadji, N.; Clark, K.; Klöckner, J.-P.; Prosenc, M.-H.; Sanvito, S.; Wiesendanger, R.; Hoffmann, G.; Hla, S.-W. Molecular Kondo Chain. *Nano Lett.* **2012**, *12* (6), 3174–3179.
- (37) Aragonès, A. C.; Aravena, D.; Cerdá, J. I.; Acís-Castillo, Z.; Li, H.; Real, J. A.; Sanz, F.; Hihath, J.; Ruiz, E.; Díez-Pérez, I. Large Conductance Switching in a Single-Molecule Device through Room

- Temperature Spin-Dependent Transport. Nano Lett. 2016, 16 (1), 218-226.
- (38) Herrmann, C. Electronic Communication as a Transferable Property of Molecular Bridges? *J. Phys. Chem. A* **2019**, *123* (47), 10205–10223.
- (39) Sierda, E.; Abadia, M.; Brede, J.; Elsebach, M.; Bugenhagen, B.; Prosenc, M. H.; Bazarnik, M.; Wiesendanger, R. On-Surface Oligomerization of Self-Terminating Molecular Chains for the Design of Spintronic Devices. ACS Nano 2017, 11 (9), 9200–9206.
- (40) Bazarnik, M.; Bugenhagen, B.; Elsebach, M.; Sierda, E.; Frank, A.; Prosenc, M. H.; Wiesendanger, R. Toward Tailored All-Spin Molecular Devices. *Nano Lett.* **2016**, *16* (1), 577–582.
- (41) Chappert, C.; Fert, A.; Van Dau, F. N. The Emergence of Spin Electronics in Data Storage. *Nat. Mater.* **2007**, *6* (11), 813–823.
- (42) Song, Z.; Sun, C. P. Quantum Information Storage and State Transfer Based on Spin Systems. *Low Temp. Phys.* **2005**, *31* (8), 686–694.
- (43) Molnár, G.; Rat, S.; Salmon, L.; Nicolazzi, W.; Bousseksou, A. Spin Crossover Nanomaterials: From Fundamental Concepts to Devices. *Adv. Mater.* **2018**, *30* (5), No. 1703862.
- (44) Frank, P.; Djuric, T.; Koini, M.; Salzmann, I.; Rieger, R.; Müllen, K.; Resel, R.; Koch, N.; Winkler, A. Layer Growth, Thermal Stability, and Desorption Behavior of Hexaaza-Triphenylene-Hexacarbonitrile on Ag(111). *J. Phys. Chem. C* **2010**, *114* (14), 6650–6657.
- (45) Zahl, P.; Wagner, T. GXSM Smart & Customizable SPM Control. GIT Imaging Microsc. 2015, 17, 38.
- (46) Zahl, P.; Klust, A. Gxsm Software Project Homepage, 2022. http://gxsm.sourceforge.net.
- (47) Microscopy | Instruments. Soft dB. https://www.softdb.com/scanning-probe-microscopy/ (accessed November 28, 2022).
- (48) Blöchl, P. E. Projector Augmented-Wave Method. *Phys. Rev. B* **1994**, *50* (24), 17953–17979.
- (49) Kresse, G.; Furthmüller, J. Efficient Iterative Schemes for *Ab Initio* Total-Energy Calculations Using a Plane-Wave Basis Set. *Phys. Rev. B* **1996**, *54* (16), 11169–11186.
- (50) Kresse, G.; Furthmüller, J. Efficiency of Ab-Initio Total Energy Calculations for Metals and Semiconductors Using a Plane-Wave Basis Set. *Comput. Mater. Sci.* **1996**, *6* (1), 15–50.
- (51) Grimme, S.; Antony, J.; Ehrlich, S.; Krieg, H. A Consistent and Accurate *Ab Initio* Parametrization of Density Functional Dispersion Correction (DFT-D) for the 94 Elements H-Pu. *J. Chem. Phys.* **2010**, 132 (15), 154104.
- (52) Steinmann, S. N.; Corminboeuf, C. A Generalized-Gradient Approximation Exchange Hole Model for Dispersion Coefficients. *J. Chem. Phys.* **2011**, 134 (4), No. 044117.
- (53) Steinmann, S. N.; Corminboeuf, C. Comprehensive Benchmarking of a Density-Dependent Dispersion Correction. *J. Chem. Theory Comput.* **2011**, 7 (11), 3567–3577.
- (54) Tersoff, J.; Hamann, D. R. Theory and Application for the Scanning Tunneling Microscope. *Phys. Rev. Lett.* **1983**, *50* (25), 1998–2001.
- (55) Yang, X.; Egger, L.; Hurdax, P.; Kaser, H.; Lüftner, D.; Bocquet, F. C.; Koller, G.; Gottwald, A.; Tegeder, P.; Richter, M.; et al. Identifying Surface Reaction Intermediates with Photoemission Tomography. *Nat. Commun.* **2019**, *10* (1), 3189.
- (56) Bumm, L. A.; Arnold, J. J.; Dunbar, T. D.; Allara, D. L.; Weiss, P. S. Electron Transfer through Organic Molecules. *J. Phys. Chem. B* 1999, 103 (38), 8122–8127.
- (57) Sautet, P. Images of Adsorbates with the Scanning Tunneling Microscope: Theoretical Approaches to the Contrast Mechanism. *Chem. Rev.* **1997**, *97* (4), 1097–1116.
- (58) Hove, M. A. V.; Cerda, J.; Sautet, P.; Bocquet, M.-L.; Salmeron, M. Surface Structure Determination by STM vs Leed. *Prog. Surf. Sci.* **1997**, *54* (3), 315–329.
- (59) Komeda, T. Spins of Adsorbed Molecules Investigated by the Detection of Kondo Resonance. *Surf. Sci.* **2014**, *630*, 343–355.
- (60) Anderson, P. W. Localized Magnetic States in Metals. *Phys. Rev.* **1961**, *124* (1), 41–53.

- (61) Li, J.; Schneider, W.-D.; Berndt, R.; Delley, B. Kondo Scattering Observed at a Single Magnetic Impurity. Phys. Rev. Lett. 1998, 80 (13), 2893-2896.
- (62) Madhavan, V.; Chen, W.; Jamneala, T.; Crommie, M. F.; Wingreen, N. S. Tunneling into a Single Magnetic Atom: Spectroscopic Evidence of the Kondo Resonance. Science 1998, 280 (5363), 567-569.
- (63) Glowatzki, H.; Bröker, B.; Blum, R.-P.; Hofmann, O. T.; Vollmer, A.; Rieger, R.; Müllen, K.; Zojer, E.; Rabe, J. P.; Koch, N. Soft" Metallic Contact to Isolated C 60 Molecules. Nano Lett. 2008, 8 (11), 3825-3829.
- (64) Müller, K.; Schmidt, N.; Link, S.; Riedel, R.; Bock, J.; Malone, W.; Lasri, K.; Kara, A.; Starke, U.; Kivala, M.; et al. Triphenylene-Derived Electron Acceptors and Donors on Ag(111): Formation of Intermolecular Charge-Transfer Complexes with Common Unoccupied Molecular States. Small 2019, 15 (33), No. 1901741.
- (65) Fano, U. Effects of Configuration Interaction on Intensities and Phase Shifts. Phys. Rev. 1961, 124 (6), 1866-1878.
- (66) Fu, Y.-S.; Ji, S.-H.; Chen, X.; Ma, X.-C.; Wu, R.; Wang, C.-C.; Duan, W.-H.; Qiu, X.-H.; Sun, B.; Zhang, P.; et al. Manipulating the Kondo Resonance through Quantum Size Effects. Phys. Rev. Lett. **2007**, 99 (25), No. 256601.
- (67) Aguiar-Hualde, J. M.; Chiappe, G.; Louis, E.; Anda, E. V. Kondo Effect in Transport through Molecules Adsorbed on Metal Surfaces: From Fano Dips to Kondo Peaks. Phys. Rev. B 2007, 76 (15), No. 155427.
- (68) Újsághy, O.; Kroha, J.; Szunyogh, L.; Zawadowski, A. Theory of the Fano Resonance in the STM Tunneling Density of States Due to a Single Kondo Impurity. Phys. Rev. Lett. 2000, 85 (12), 2557–2560.
- (69) Knorr, N.; Schneider, M. A.; Diekhöner, L.; Wahl, P.; Kern, K. Kondo Effect of Single Co Adatoms on Cu Surfaces. Phys. Rev. Lett. 2002, 88 (9), No. 096804.
- (70) Plihal, M.; Gadzuk, J. W. Nonequilibrium Theory of Scanning Tunneling Spectroscopy via Adsorbate Resonances: Nonmagnetic and Kondo Impurities. Phys. Rev. B 2001, 63 (8), No. 085404.
- (71) Maughan, B.; Zahl, P.; Sutter, P.; Monti, O. L. A. Configuration-Specific Electronic Structure of Strongly Interacting Interfaces: TiOPc on Cu(110). Phys. Rev. B 2017, 96 (23), No. 235133.
- (72) Komeda, T.; Isshiki, H.; Liu, J.; Katoh, K.; Yamashita, M. Variation of Kondo Temperature Induced by Molecule-Substrate Decoupling in Film Formation of Bis(Phthalocyaninato)Terbium(III) Molecules on Au(111). ACS Nano 2014, 8 (5), 4866-4875.
- (73) Lemes, M. A.; Magnan, F.; Gabidullin, B.; Brusso, J. Impact of Nuclearity and Topology on the Single Molecule Magnet Behaviour of Hexaazatrinaphtylene-Based Cobalt Complexes. Dalton Trans. **2018**, 47 (13), 4678–4684.
- (74) Mugarza, A.; Robles, R.; Krull, C.; Korytár, R.; Lorente, N.; Gambardella, P. Electronic and Magnetic Properties of Molecule-Metal Interfaces: Transition-Metal Phthalocyanines Adsorbed on Ag(100). Phys. Rev. B 2012, 85 (15), No. 155437.
- (75) Hapala, P.; Kichin, G.; Wagner, C.; Tautz, F. S.; Temirov, R.; Jelínek, P. Mechanism of High-Resolution STM/AFM Imaging with Functionalized Tips. Phys. Rev. B 2014, 90 (8), No. 085421.
- (76) Zhong, Q.; Li, X.; Zhang, H.; Chi, L. Noncontact Atomic Force Microscopy: Bond Imaging and Beyond. Surf. Sci. Rep. 2020, 75 (4), No. 100509.